

# Ultrasonic Image Registration for Multi-Frequency Analysis

Naomi Yagi<sup>1</sup>, Tomomoto Ishikawa<sup>2</sup>, Yutaka Hata<sup>1,3,4</sup>

<sup>1</sup>Graduate School of Engineering, University of Hyogo, Himeji, Japan

<sup>2</sup>Ishikawa Hospital, Himeji, Japan

<sup>3</sup>Himeji Initiative in Computational Medical and Health Technology, University of Hyogo, Himeji, Japan,

<sup>4</sup>WPI Immunology Frontier Research Center, Osaka University, Osaka, Japan,

Email: naomi.yagi@ieee.org

Received June 26, 2013; revised July 26, 2013; accepted August 3, 2013

Copyright © 2013 Naomi Yagi *et al.* This is an open access article distributed under the Creative Commons Attribution License, which permits unrestricted use, distribution, and reproduction in any medium, provided the original work is properly cited.

## ABSTRACT

This paper describes ultrasonic image registration for multi-frequency analysis. The goal of our research is the portable and real time brain diagnosis under the thick-skull. The choice of ultrasonic frequency is a trade-off between spatial image resolution and imaging depth. This study shows the usability of data synthesis by employing two different frequency ultrasounds. In the first part of this study, using Fast Fourier Transform, we conclude that the synthesized image was produced from two ultrasonic images of individual objects. The purpose of the second approach of the data synthesis is to investigate three methods of ultrasonic imaging. This approach is particular interest for the design of further study intending to visualize any defects by ultrasonic methods. As the results, the synthesized image with Wavelet transform has higher efficiency than the other synthesized ones for the bone and the sulcus. In summary, this study indicates that the ultrasonic synthesized image is useful to visualize the imitated brain area. This observation is encouraging for further studies of evaluating brain for patients.

**Keywords:** Ultrasound; Human Brain; Data Synthesis; Fourier Transform; Wavelet Transform

## 1. Introduction

Ultrasound has been used to image the human body and has become one of the most widely used diagnostic tools in modern medicine. The technology is relatively inexpensive and portable, especially when compared with other modalities, such as magnetic resonance imaging (MRI) and computed tomography (CT), which are time-consuming, and require radioactive tracers. Ultrasound is also used to visualize tissue during routine and emergency prenatal care. As currently applied in the medical field, properly performed ultrasound poses no known risks to the patient. Moreover, it has been shown that it is possible to visualize and measure changes in ultrasound intensities with the use of harmonic gray-scale ultrasound imaging [1-3].

Though the frequency up to 50 - 100 MHz has been experimentally used in a technique known as biomicroscopy in special regions, typical diagnostic sonographic scanners operate in the frequency range of 2 - 18 MHz [3]. In the bone, the ultrasound causes large absorption and scattering, so the ultrasonic device is rarely used to

the bone. The bone tissue has higher attenuation than the other tissue. Therefore, the general ultrasonic devices are not available for transmitting bone tissue. In Reference [4], the transcranial sonography has been proposed using two linear array probes. These ultrasonic array probes consist of 128 elements. However, it is difficult to transmit ultrasound from the random position because the two array probes are set up on both sides of human head. In Reference [5], they employ the spherical array probe that consists of the 448 elements. However, they only described a signal processing. We proposed an imaging system of the skull and brain surface using a 1.0 MHz single ultrasonic probe [6,7]. In this system, it was scanned a target object at the interval of 1.0mm with a 3-D scanner. It is difficult to apply to clinical practice because this scanner is too large to use and constrains human head. Therefore, a simple and unrestrained system without the large mechanical scanner is strongly required. We proposed the transcranial brain imaging system by using ultrasonic array probe [8,9]. On the other hand, in the case of employing wideband ultrasound, it is difficult to make a sector scan system on structural design. Thus,

the frequency analysis is useful using multiple ultrasonic waves.

In this study, we propose ultrasonic image registration for multi-frequency analysis. In our experiment, we used a cow scapula as a skull and a steel sulcus as a cerebral sulcus. To obtain the high-quality image by taking each advantage of two alternative frequency waves, we proposed some synthesizing methods using statistic resonance [10-15], Fourier Transform, and Wavelet Transform [16-19]. This study extended our works in [20-22]. As the results, we obtained the clearest ultrasonic image when synthesizing with Wavelet transform. This result is superior to the other synthesized ones.

## 2. Experimental Environments

The most defective point of the ultrasonic wave is impossible to pass through the bone. Thus far, the brain diagnosis had not used the ultrasonic devices. But currently, the ultrasonic performance have improved, the ultrasonic wave passing through the temple enables the brain diagnosis. We describe an imaging method for the human cerebral sulcus using two ultrasonic array probes with the center frequency of 0.5 MHz and 1.0 MHz to extract the surface of the bone and the sulcus. Our experiment indicates with a pink square in **Figure 1**.

In this study, we employ a cow scapula as a skull and a steel sulcus as a cerebral sulcus. Because the average thickness of human skull is about 3.0 mm, we employ the part of the cow scapula about 2.6 mm.

### 2.1. Experimental Materials

The cow scapula is shown in **Figure 2**. The thickness of

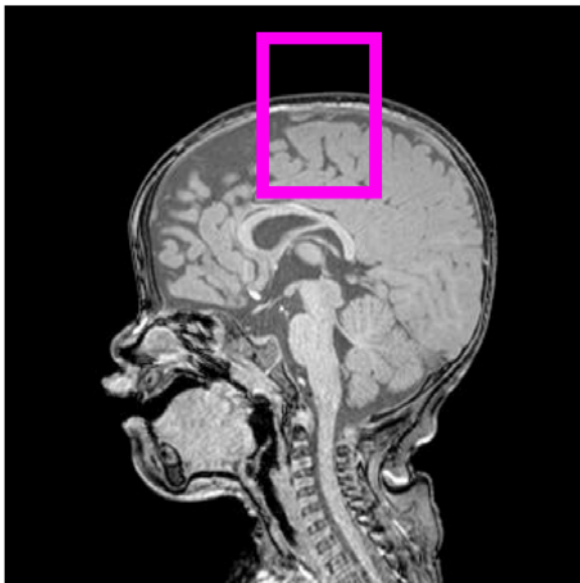


**Figure 1. Target-human brain.**

the point A is 2.64 mm and the thickness of the point B is 11.18 mm. The width is 110.0 mm. In this experiment, we employ the point A.

As a cerebral sulcus, we employ a steel sulcus as shown in **Figures 3**. **Table 1** shows the specification of the steel sulcus. We employed the steel sulcus of No. 2.

### 2.2. Ultrasonic Device

We employ 1.0 MHz array probe (ISL Inc., ISL1938) 0.5 MHz array probe (ISL Inc., ISL2022) as shown in **Figures 4(a)** and **(b)**. The center frequency of ISL1938 is 1.0 MHz and that of ISL2022 is 0.5 MHz. **Figure 5** shows the system of these array probes. Both array probes consist of 32 elements at intervals of 1.5 mm. On the other hand, the ultrasound transducer size of 1.0 MHz is 24 mm × 1.5 mm × 32 ch, the one of 0.5 MHz is 30 mm × 1.5 mm × 32 ch. If a wideband ultrasonic transducer is

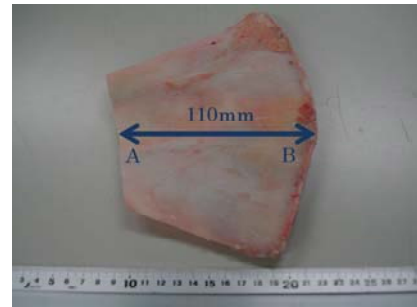


**Figure 2. Cow scapula.**

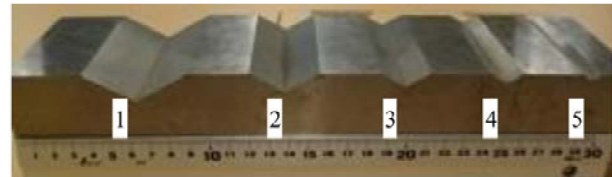


**Figure 3. Steel sulcus.**

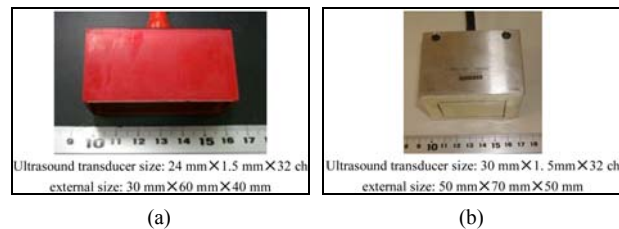


**Figure 4. Ultrasonic array probe. (a) 1.0 MHz (ISL1938); (b) 0.5 MHz (ISL2022).**

**Table 1. Specification of steel sulcus.**

Sulcus	1	2	3	4	5
Width [mm]	51.96	34.64	24.25	17.32	10.39
Depth [mm]	15.00	10.00	7.00	5.00	3.00

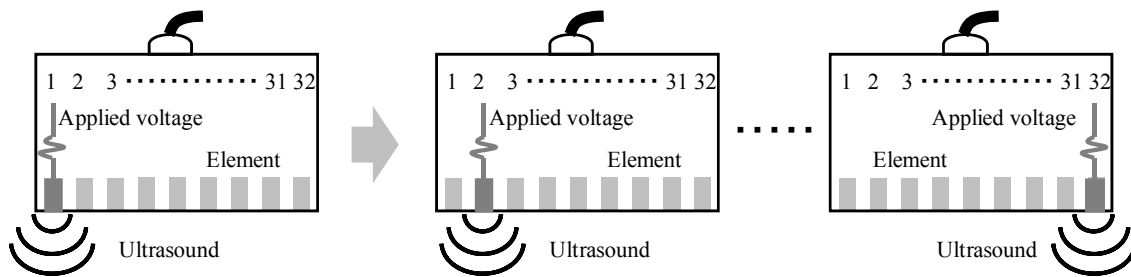


Figure 5. System of array probe (Electronic control shift).

employed, it is difficult to make a sector scan system on structural design. The voltage is applied to the element and the ultrasound is generated from the element. The applied voltage shifts by one element and the ultrasound is generated. The array probe can obtain 32 ultrasonic waveforms inline.

### 2.3. Data Acquisition System

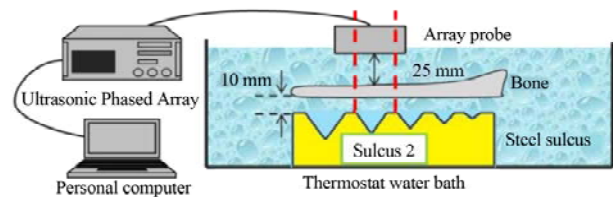
Our ultrasonic data acquisition system is shown in **Figure 6(a)**. The cow scapula and the steel sulcus are placed in a thermostat water bath. In this experiment, water temperature is adjusted to 20°C by a thermostat water bath (Thomas Kagaku Co. Ltd., T-22L). The distance between the array probe and the cow scapula is about 25 mm. The distance between the cow scapula and the steel sulcus is about 10 mm. The ultrasonic phased array (Ei-shin Kagaku Co. Ltd., MC-64) transmits and receives ultrasonic waves via the array probe. The pulse repetition frequency (PRF) is 50 MHz. In this experiment, we can obtain the ultrasonic waves from the random position by manual-scanning of the ultrasonic array probe. We obtain 32 data at once.

**Figures 6(b)** and **(c)** are the B-mode images which are ultrasonic images by using 1.0 MHz and 0.5 MHz ultrasonic array probes.

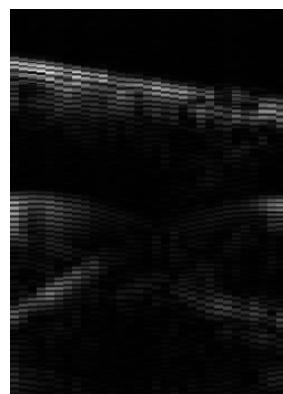
### 3. Preliminary

The most defective point of the ultrasonic wave is impossible to pass through the bone. Thus far, the brain diagnosis had not used the ultrasonic devices. But currently, the ultrasonic performance have improved, the ultrasonic wave passing through the temple enables the brain diagnosis. We describe an imaging method for the human cerebral sulcus using two ultrasonic array probes with the center frequency of 1.0 MHz and 0.5 MHz to extract the surface of the bone and the sulcus.

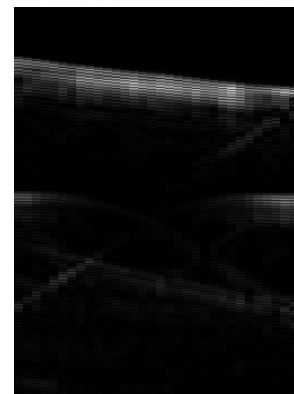
In order to improve the ultrasonic raw image, we propose the ultrasonic data synthesis method. As preliminary experiment, we synthesize the images which are measured the bone and the sulcus, individually. Firstly, we measured the bone by using 1.0 MHz ultrasonic probe in **Figure 7(a)**. Secondly, we we measured the



(a)



(b)



(c)

Figure 6. Ultrasonic data system. (a) Data Acquisition System; (b) B-mode Image by using 1.0 MHz; (c) B-mode Image by using 0.5 MHz.

sulcus by using 0.5 MHz ultrasonic probe in **Figure 7(b)**. The ultrasonic images of the bone and the sulcus are **Figures 7(c)** and **(d)**, respectively.

With these ultrasonic images, we proposed the ultrasonic data synthesis by applying the Fourier transform. The Fourier transform is a mathematical operation that decomposes a signal into its constituent frequencies. The original signal depends on time, and therefore it is called the time domain representation of the signal, whereas the Fourier transform depends on frequency and is called the frequency domain representation of the signal. The term Fourier transform refers both to the frequency domain representation of the signal and the process that transforms the signal to its frequency domain representation. It is also possible to generalize the Fourier transform on discrete structures such as finite groups. The efficient computation of such structures, by fast Fourier transform, is essential for high-speed computing. In our study, we

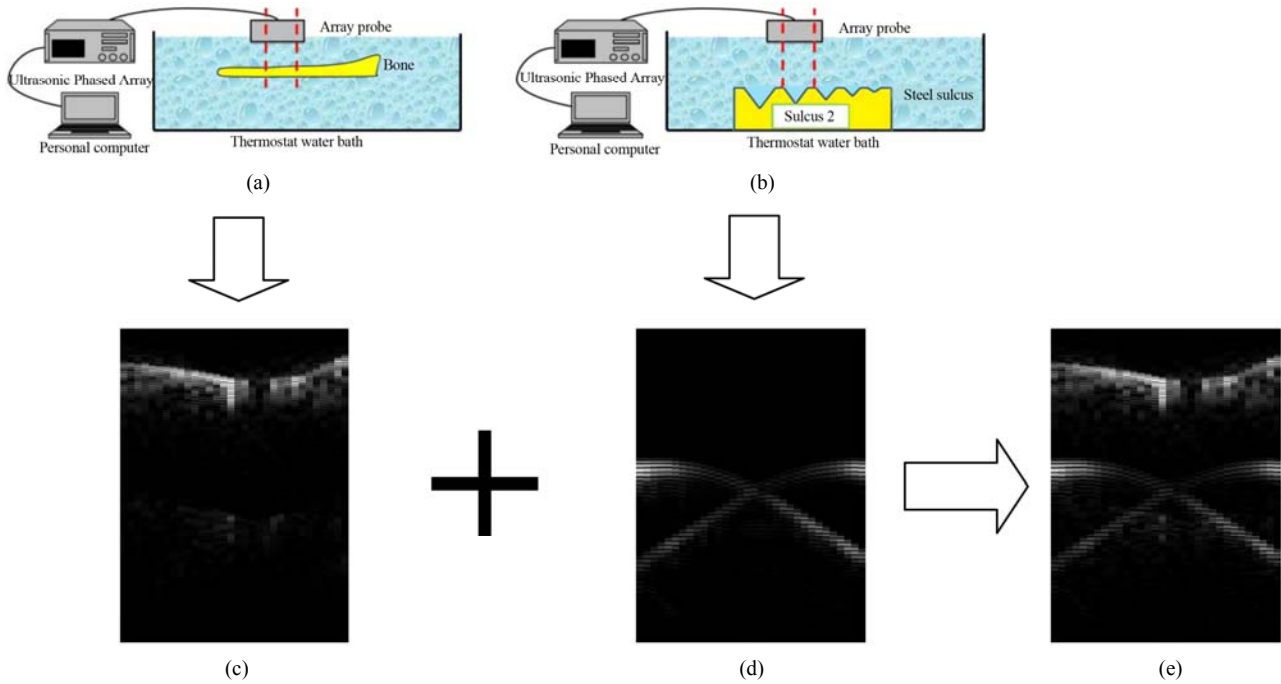


**Figure 7.** FFT Synthesized Image of Bone and Steel Sulcus. (a) Measurement of Bone by using 1.0 MHz; (b) Measurement of Steel Sulcus by using 0.5 MHz; (c) Raw Image of Bone; (d) Raw Image of Steel Sulcus; (e) Synthesized Image.

use fast Fourier transform for the purpose of fast processing.

We apply the fast Fourier transform to 1.0 MHz ultrasonic data of the bone image and 0.5 MHz ultrasonic data of the sulcus image using Equation (1), respectively.

$$f_j = \sum_{k=0}^{N-1} x_k e^{\left(-\frac{2\pi ijk}{N}\right)} \quad j = 0, \dots, N-1 \quad (1)$$

After applying fast Fourier transform, we synthesized the ultrasonic data of 1.0 MHz and 0.5 MHz on complex number. Then, we apply the inverse Fourier transform to the synthesized data using Equation (2).

$$x_k = \frac{1}{N} \sum_{j=0}^{N-1} f_j e^{\left(\frac{2\pi ijk}{N}\right)} \quad j = 0, \dots, N-1 \quad (2)$$

**Figure 7(e)** shows the image obtained by the inverse Fourier transform data. We define this image as the FFT synthesized image. Judging from this synthesized image, it was demonstrated the ultrasonic data synthesis by fast Fourier transform.

On the other hand, we apply the FFT method to tofu as biological phantom in **Figures 8(a)** and **(b)**. In our study, the raw images of the bone and the tofu are obtained respectively as shown in **Figures 8(c)** and **(d)**. The image of the bone is obtained by 1.0 MHz ultrasonic array probe. The other one of the tofu is obtained by 0.5 MHz ultrasonic array probe. **Figure 8(e)** shows the synthesized image.

## 4. Ultrasonic Data Synthesis

To improve the ultrasonic image quality, we proposed the ultrasonic data synthesis. We employ the ultrasonic data which both the bone and the sulcus are set as shown in **Figure 6**. The flowchart of the proposed system is shown in **Figure 9**. This system consists of three methods. In the first method, we synthesized the data of 1.0 MHz and 0.5 MHz by using statistic resonance. In the second method, we synthesized the data by using the Fourier transform. Lastly, we synthesized the data by using Wavelet transform. These methods never change each frequency component.

### 4.1. Fourier Transform

The Fourier transform is the useful tool to analyze the frequency components of the signal and decomposes a signal into its constituent frequencies. The original signal depends on time, and therefore it is called the time domain representation of the signal, whereas the Fourier transform depends on frequency and is called the frequency domain representation of the signal. The term Fourier transform refers both to the frequency domain representation of the signal and the process that transforms the signal to its frequency domain representation. It is also possible to generalize the Fourier transform on discrete structures such as finite groups. The efficient computation of such structures, by the Fourier transform, is essential for high-speed computing. In our study, we use the Fourier transform for the purpose of fast proc-

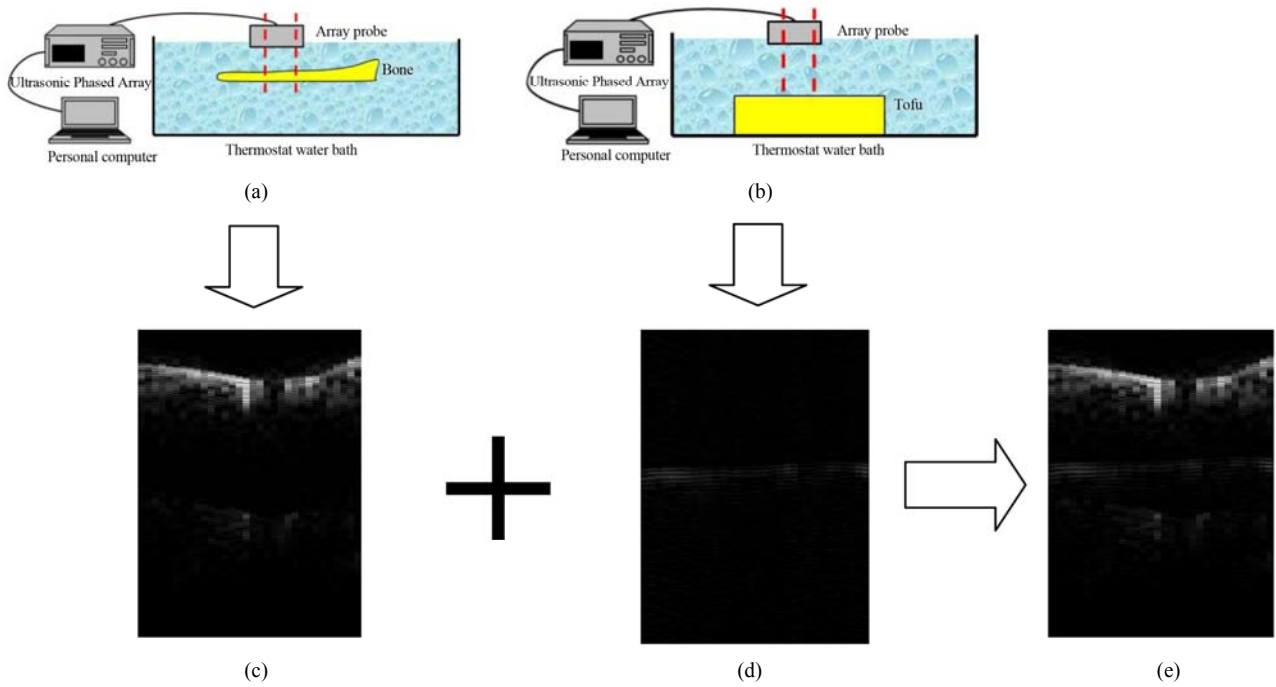


**Figure 8. FFT Synthesized Image of Bone and Tofu. (a) Measurement of Bone by using 1.0 MHz; (b) Measurement of Tofu by using 0.5 MHz; (c) Raw Image of Bone; (d) Raw Image of Tofu; (e) Synthesized Image.**

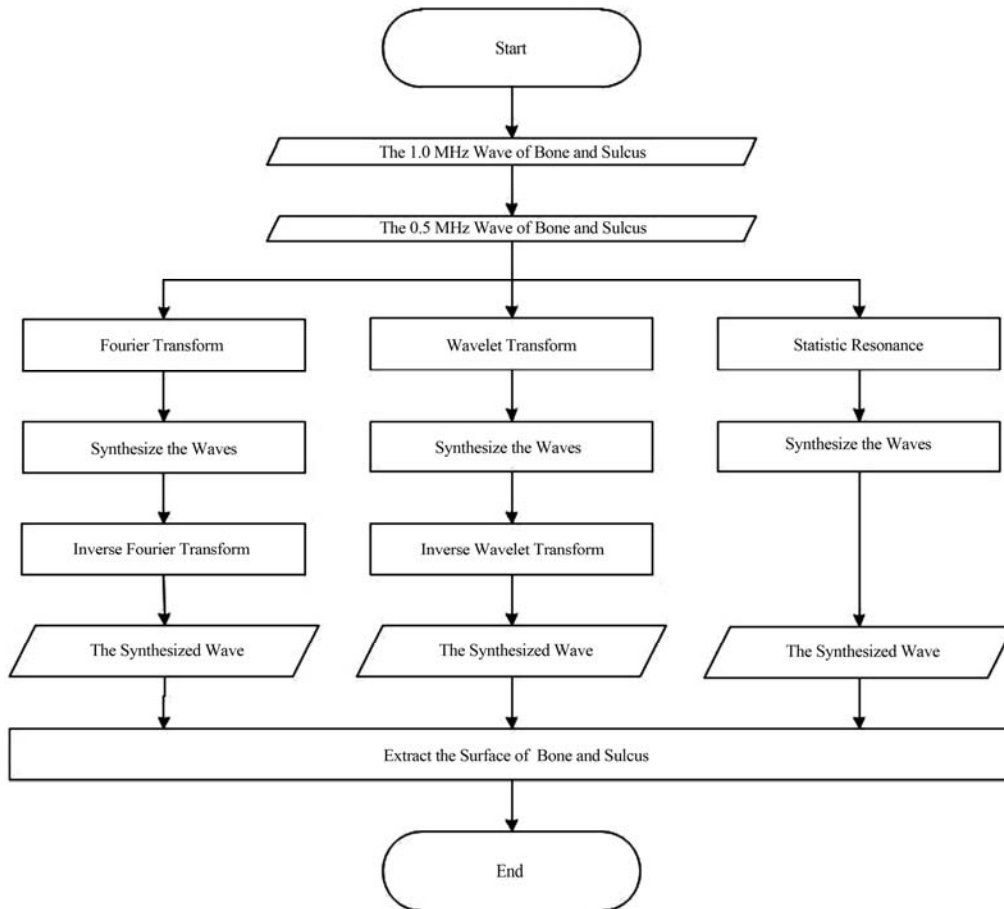


**Figure 9. Flowchart of the proposed system.**



essing.

The detail processing is described in the previous section. At First, we obtained two ultrasonic waves for the center frequency of 1.0 MHz and 0.5 MHz. To each wave, we perform the Fourier transform. We synthesized the data after performing the Fourier transform. Then, we apply the inverse Fourier transform to the synthesized data. **Figure 11(a)** shows the image obtained by the inverse Fourier transform data. We define this image as the FFT synthesized image.

## 4.2. Wavelet Transform

The Wavelet transform is a computational tool for a variety of signal and image processing applications. For example, the Wavelet transform is useful for the compression of digital image files; smaller files are important for storing images using less memory and for transmitting images faster and more reliably. The Wavelet transform covers the problems which the Fourier transform has as follows. If we take the Fourier transform over the whole time axis, we cannot define at what instant a particular frequency rises. The Short-time Fourier transform (STFT) uses a sliding window to find spectrogram, which gives the information of both time and frequency. Another problem exists that the length of window limits the resolution in frequency. The Wavelet transform is based on small wavelets with limited duration and allow us to analyze the signal in different scale.

By using two ultrasonic waves for the center frequency of 1.0 MHz and 0.5 MHz, we apply the Wavelet transform using Equations (3) and (4).

$$\psi_{jk}(x) = 2^{j/2} \psi(2^j x - k) \quad (3)$$

$$WA(x) = \sum_{j,k=-\infty}^{\infty} c_{jk} \psi_{jk}(x) \quad (4)$$

The wavelet coefficient  $c_{jk}$  is then given by Equation (5).

$$c_{jk} = (W_{\psi} f)(2^{-j}, k2^{-j}) \quad (5)$$

Passing through the Wavelet transform, we obtain the outputs giving the detail coefficients from the high-pass filter and approximation coefficients from the low-pass filter as shown in **Figure 10**.

**Figure 11(b)** shows the image obtained by applying inverse Wavelet transform to the synthesized data after performing Wavelet transform to each data.

## 4.3. Statistic Resonance

We synthesize the waves of 1.0 MHz and 0.5 MHz by employing statistic resonance. We add the waves obtained by the 1.0 MHz array probe to the waves by the 0.5 MHz array probe using Equation (6). In this study,

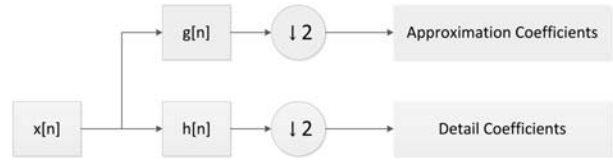


**Figure 10. Block diagram of filter analysis.**

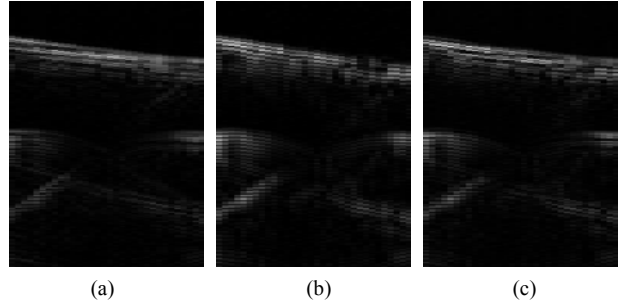


**Figure 11. Synthesized images. (a) Fourier Transform; (b) Wavelet Transform; (c) Statistic Resonance.**

the value “ratio” is 0.5. The notations  $f(x,y)$  and  $g(x,y)$  denote the amplitudes of ultrasonic waves obtained by the array probe of 1.0 MHz and those of 0.5 MHz, respectively, where  $(x,y)$  denotes the coordinate of ultrasonic B-mode image. We show the synthesized image by using statistic resonance in **Figure 11(c)**.

$$h(x, y) = \text{ratio} \times f(x, y) + (1 - \text{ratio}) \times g(x, y) \quad (6)$$

## 5. Experimental Results

We applied the synthesized methods to the ultrasonic images and indicated the validity of synthesizing the waves of two alternative frequencies using ultrasonic data of a cow scapula as a skull and a steel sulcus as a cerebral sulcus. The sulcus was placed in the thermostat water bath. We set the cow scapula between the array probe and the steel sulcus. In this experiment, we performed three synthesizing methods. After applying each method, we extract the sulcus surface of the image. As the results, we compared each image with the only sulcus image in **Figure 7(b)**, which is defined as the true image. **Figure 12** is the results with the extracted images. The light-blue bars show the pixel numbers of FP and FN, and the blue bars show the pixel numbers of FP. The rate of FP and FN is approximate 5% or less. Judging from this figure, it is indicated that the synthesizing method using the Wavelet transform is superior to the other methods. The image of the bone and the sulcus with the

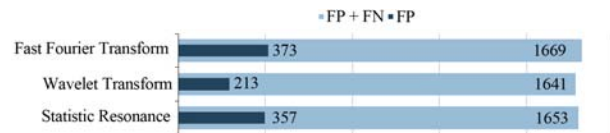


**Figure 12. Results with extract image.**

Wavelet transform was the clearest for all the images. The Wavelet transform has the basis function with automatic scaling, and thus enables to analyze the wide range frequency. For synthesizing the ultrasonic images, the Wavelet transform is more effective synthesis method.

## 6. Conclusions

In this paper, we proposed an ultrasonic image synthesis by using two ultrasonic array probes with the each center frequency of 1.0 MHz and 0.5 MHz. In the preliminary experiment, the images of the individual objects were synthesized by using FFT. As biological phantom, the tofu was employed. With the synthesized images, the synthesis is useful for the ultrasonic images. This study performed the experiment using a cow scapula as a skull and a steel sulcus as a cerebral sulcus. As the results, we obtained the clearest synthesized image using Wavelet transform. This result is superior to the results of other synthesized images. The Wavelet transform will be useful for the ultrasonic waves.

The choice of frequency is a trade-off between spatial resolution of the image and imaging depth. Lower frequency produces less resolution but image deeper into the body. Higher frequency sound waves have a smaller wavelength and thus are capable of reflecting or scattering from smaller structures. In the bone, the ultrasound causes large absorption and scattering, so the ultrasonic device is rarely used to the bone. The bone tissue has higher attenuation than the other tissue. Therefore, the general ultrasonic devices are not available for transmitting bone tissue. However, we can transmit the low frequency under 1.0 MHz to bone tissue. In clinical practice, the ultrasonic device with the center frequency of 0.5 MHz is performed to diagnose osteoporosis. In this work, we indicated the superiority to synthesize the ultrasonic images of different frequencies.

In the future, the sparse decoding and PCA will apply to this system. It will be meaningful for human brain ultrasound-mediated diagnosis in the near future. On the other hand, the sparse coding is available to learn the basis function for each tissue. The component is incorporated and computed the coefficient of the basis function. When this system is achieved, it is very useful for human brain ultrasound-mediated diagnosis.

Our future work is an implementation of a mobile application and performing our technology on the actual medical products for home health care.

## REFERENCES

- [1] K. A. Wear, "Autocorrelation and Cepstral Methods for Measurement of Tibial Cortical Thickness," *IEEE Transactions on Ultrasonics, Ferroelectrics, and Frequency Control*, Vol. 50, No. 5, 2003, pp. 655-660.
- [2] J. Krautkramer and H. Krautkramer, "Ultrasonic Testing of Materials," Springer-Verlag, Berlin, 1990. [doi:10.1007/978-3-662-10680-8](https://doi.org/10.1007/978-3-662-10680-8)
- [3] G. Seidel, C. Algermissen, A. Christoph, L. Claassen, M. Vidal-Langwasser and T. Katzer, "Harmonic Imaging of the Human Brain: Visualization of Brain Perfusion with Ultrasound," *Stroke*, Vol. 31, No. 1, 2000, pp. 151-154. [doi:10.1161/01.STR.31.1.151](https://doi.org/10.1161/01.STR.31.1.151)
- [4] T. R. Nelson, *et al.*, "Three-Dimensional Ultrasound," Lippincott Williams and Wilkins, Philadelphia, 1999.
- [5] F. Vignon, J.-F. Aubry, M. Tanter, A. Margoum and M. Fink, "Dual-Arrays Brain Imaging Prototype: Experimental In Vitro Results," *IEEE International Ultrasonics Symposium*, Vol. 1, 18-21 September 2005, pp. 504-507.
- [6] P. J. White, G. T. Clement and K. Hynynen, "Transcranial Ultrasound Focus Reconstruction with Phase and Amplitude Correction," *IEEE Transactions on Ultrasonics, Ferroelectrics, and Frequency Control*, Vol. 52, No. 9, 2005, pp. 1518-1522. [doi:10.1109/TUFFC.2005.1516024](https://doi.org/10.1109/TUFFC.2005.1516024)
- [7] Y. Hata, S. Kobashi, K. Kondo, Y. T. Kitamura and T. Yanagida, "Transcranial Ultrasonography System for Visualizing Skull and Brain Surface Aided by Fuzzy Expert System," *IEEE Transactions on Systems, Man and Cybernetics*, Vol. 35, No. 6, 2005, pp. 1360-1373. [doi:10.1109/TSMCB.2005.855593](https://doi.org/10.1109/TSMCB.2005.855593)
- [8] M. Kimura, S. Kobashi, K. Kondo, Y. Hata, Y. T. Kitamura and T. Yanagida, "Fuzzy Ultrasonic Imaging System for Visualizing Braine Surface under Skull Considering Ultrasonic Refraction," *Proceedings of 2006 IEEE International Conference on Systems, Man, and Cybernetics*, Montreal, 7-10 October 2007, pp. 3790-3794.
- [9] Y. Ikeda, S. Kobashi, K. Kondo and Y. Hata, "Fuzzy Ultrasonic Array System for Locating Screw Holes of Intramedullary Nail," *Proceedings of 2006 IEEE International Conference on Systems, Man, and Cybernetics*, Montreal, 7-10 October 2007, pp. 3428-3432.
- [10] M. D. McDonnell and D. Abbott, "What Is Stochastic Resonance? Definitions, Misconceptions, Debates, and Its Relevance to Biology," *PLoS Computational Biology*, Vol. 5, No. 5, 2009, p. e1000348. [doi:10.1371/journal.pcbi.1000348](https://doi.org/10.1371/journal.pcbi.1000348)
- [11] T. Mori and S. Kai, "Noise-Induced Entrainment and Stochastic Resonance in Human Brain Waves," *Physical Review Letters*, Vol. 88, 2002, Article ID. 218101. [doi:10.1103/PhysRevLett.88.218101](https://doi.org/10.1103/PhysRevLett.88.218101)
- [12] P. Hänggi, "Stochastic Resonance in Biology—How Noise Can Enhance Detection of Weak Signals and Help Improve Biological Information Processing," *ChemPhys-Chem*, Vol. 3, No. 3, 2002, pp. 285-290. [doi:10.1002/1439-7641\(20020315\)3:3<285::AID-CPHC285>3.0.CO;2-A](https://doi.org/10.1002/1439-7641(20020315)3:3<285::AID-CPHC285>3.0.CO;2-A)
- [13] L. Ke, X. Jianping, K. Dongmei and Z. Na, "A Method of Evaluating the Signal to Noise Ratio Based on Duffing Time Series," *Proceedings of the 2009 International Conference on Measuring Technology and Mechatronics Automation*, Zhangjiajie, Vol. 1, 11-12 April 2009, pp. 399-402.

- [14] Y. Hotta, T. Kanki, N. Asakawa, H. Tabata and T. Kawai, "Cooperative Dynamics of an Artificial Stochastic Resonant System," *Applied Physics Express*, Vol. 1, 2008, Article ID. 088002.
- [15] K. Wiesenfeld and F. Jaramillo, "Minireview of Stochastic Resonance," *Chaos* 8, 1998, pp. 539-548. [doi:10.1063/1.166335](https://doi.org/10.1063/1.166335)
- [16] G. Hiramatsu, Y. Ikeda, S. Imawaki, Y. T. Kitamura, T. Yanagida, S. Kobashi and Y. Hata, "Trans-Skull Imaging System by Ultrasonic Array Probe," *Proceedings of 2009 IEEE International Conference on Systems, Man and Cybernetics*, 11-14 October 2009, pp. 1096-1101. [doi:10.1109/ICSMC.2009.5345974](https://doi.org/10.1109/ICSMC.2009.5345974)
- [17] N. Yagi, Y. Oshiro, O. Ishikawa, Y. Hata, Y. T. Kitamura and T. Yanagida, "YURAGI: Analysis for Trans-Skull Brain Visualizing by Ultrasonic Array Probe," *Proceedings of SPIE Defence, Security and Sensing*, 2011, pp. 805813-1-9.
- [18] N. Yagi, Y. Oshiro, O. Ishikawa, G. Hiramatsu, Y. Hata, Y. Kitamura and T. Yanagida, "Data Synthesis for Trans-Skull Brain Imaging by 0.5 and 1.0MHz Ultrasonic Array Systems," *Proceedings of 2010 IEEE International Conference on Systems, Man and Cybernetics*, Istanbul, 10-13 October 2010, pp. 1524-1529. [doi:10.1109/ICSMC.2010.5642325](https://doi.org/10.1109/ICSMC.2010.5642325)
- [19] G. Hiramatsu, S. Kobashi, Y. Hata and S. Imawaki, "Ultrasonic Large Intestine Thickness Determination System for Low Anterior Resection," *Proceedings of 2008 IEEE International Conference on Systems, Man and Cybernetics*, Singapore, 12-15 October 2008, pp. 3072-3076. [doi:10.1109/ICSMC.2008.4811767](https://doi.org/10.1109/ICSMC.2008.4811767)
- [20] N. Yagi, Y. Oshiro, T. Ishikawa and Y. Hata, "Ultrasonic Image Synthesis in Fourier Transform," *Proceedings of 2012 World Automation Congress*, Puerto Vallarta, 24-28 June 2012, pp. 1-6.
- [21] N. Yagi, Y. Oshiro, T. Ishikawa and Y. Hata, "Human Brain Ultrasound-Mediated Diagnosis in Emergency Medicine and Home Health Care," *Proceedings of the 6th International Conference on Soft Computing and Intelligent Systems and 13th International Symposium on Advanced Intelligent Systems*, 20-24 November 2012, pp. 1269- 1274. [doi:10.1109/SCIS-ISIS.2012.6505270](https://doi.org/10.1109/SCIS-ISIS.2012.6505270)
- [22] N. Yagi, Y. Oshiro, T. Ishikawa, and Y. Hata, "Yuragi Synthesis for Ultrasonic Human brain Imaging," *Journal of Advanced Computational Intelligence and Intelligent Informatics*, Vol. 17, No. 1, 2013, pp. 74-82.